Available online at www.sciencedirect.com
SCIENCE DIRECT®
Electric Power Systems Research 69 (2004) 129–141
ELECTRIC POWER SYSTEMS RESEARCH
www.elsevier.com/locate/epsr

Robust coordinated design of excitation and TCSC-based stabilizers using genetic algorithms

Y.L. Abdel-Magid*, M.A. Abido

Electric Engineering Department, King Fahd University of Petroleum & Minerals, Dhahran 31261, Saudi Arabia

Received 19 November 2002; accepted 18 September 2003

Abstract

Power system stability enhancement via robust coordinated design of a power system stabilizer (PSS) and a thyristor-controlled series capacitor (TCSC)-based stabilizer is thoroughly investigated in this paper. The coordinated design problem of robust excitation and TCSC-based controllers over a wide range of loading conditions and system configurations is formulated as an optimization problem with an eigenvalue-based objective function. The real-coded genetic algorithm (RCGA) is employed to search for optimal controller parameters. This study also presents a singular value decomposition (SVD)-based approach to assess and measure the controllability of the poorly damped electromechanical modes by different control inputs. The damping characteristics of the proposed control schemes are also evaluated in terms of the damping torque coefficient over a wide range of loading conditions. The proposed stabilizers were tested on a weakly connected power system. The damping torque coefficient analysis, nonlinear simulation results, and eigenvalue analysis show the effectiveness and robustness of the proposed approach over a wide range of loading conditions.

Keywords: Power system stabilizer; FACTS devices; TCSC; Real-coded genetic algorithms

1. Introduction

Since 1960s, low frequency oscillations have been observed when large power systems are interconnected by relatively weak tie lines. These oscillations may sustain and grow to cause system separation if no adequate damping is available [1,2]. Nowadays, the conventional power system stabilizer (CPSS) is widely used by power system utilities.

Generally, it is important to recognize that machine parameters change with loading making the machine behavior quite different at different operating conditions. Since these parameters change in a rather complex manner, a set of stabilizer parameters which stabilize the system under a certain operating condition may no longer yield satisfactory results when there is a drastic change in power system operating conditions and configurations. Hence, PSSs should provide some degree of robustness to the variations in system parameters, loading conditions, and configurations.

H_∞ optimization techniques [3,4] have been applied to robust PSS design problem. However, the importance and difficulties in the selection of weighting functions of the H_∞ optimization problem have been reported. In addition, the additive and/or multiplicative uncertainty representation cannot treat situations where a nominal stable system becomes unstable after being perturbed [5]. Moreover, the pole-zero cancellation phenomenon associated with this approach produces closed loop poles whose damping is directly dependent on the open loop system (nominal system) [6]. On the other hand, the order of the H_∞-based stabilizer is as high as that of the plant. This gives rise to complex structure of such stabilizers and reduces their applicability.

Kundur et al. [7] have presented a comprehensive analysis of the effects of the different CPSS parameters on the overall dynamic performance of the power system. It is shown that the appropriate selection of CPSS parameters results in satisfactory performance during system upsets. In addition, Gibbard [8] demonstrated that the CPSS provides satisfactory damping performance over a wide range of system loading conditions. Robust design of CPSSs in multimachine power systems using genetic algorithms is presented in [9] where

* Corresponding author. Tel.: +966-3-860-2244; fax: +966-3-860-3535.
E-mail address: amagid@kfupm.edu.sa (Y.L. Abdel-Magid).

0378-7796/$ – see front matter © 2003 Elsevier B.V. All rights reserved.
doi:10.1016/j.epsr.2003.06.009

several loading conditions are considered in the design process.

Although PSSs provide supplementary feedback stabilizing signals, they suffer a drawback of being liable to cause great variations in the voltage profile and they may even result in leading power factor (pf) operation under severe disturbances. The recent advances in power electronics have led to the development of the flexible alternating current transmission systems (FACTS). Generally, a potential motivation for the accelerated use of FACTS devices is the deregulation environment in contemporary utility business. Along with primary function of the FACTS devices, the real power flow can be regulated to mitigate the low frequency oscillations and enhance power system stability.

Recently, several FACTS devices have been implemented and installed in practical power systems [10,11]. In the literature, a little work has been done on the coordination problem investigation of excitation and FACTS-based stabilizers. Noorozian and Anderson [12] presented a comprehensive analysis of damping of power system electromechanical oscillations using FACTS where the impact of transmission line loading and load characteristics on the damping effect of these devices have been discussed. Wang and Swift [13] have discussed the damping torque contributed by FACTS devices where several important points have been analyzed and confirmed through simulations. However, all controllers were assumed proportional and no efforts have been done towards the controller design. On the other hand, it is necessary to measure the electromechanical mode controllability in order to assess the effectiveness of different controllers and form a clear inspiration about the coordination problem requirements. A comprehensive study of the coordination problem requirements among PSSs and different FACTS devices has been presented in [14]. However, no efforts have been done towards the coordinated design of the stabilizers.

A considerable attention has been directed for investigating the effect of thyristor-controlled series capacitor (TCSC) on power system stability [15–23]. Several approaches based on modern control theory have been applied to TCSC controller design. Chen et al. [15] presented a state feedback controller for TCSC by using a pole placement technique. However, the controller requires all system states. This reduces its applicability in real-life power systems. Chang and Chow [16] developed a time optimal control strategy for the TCSC where a performance index of time was minimized. A fuzzy logic controller for a TCSC was proposed in [17]. The impedance of the TCSC was adjusted based on machine rotor angle and the magnitude of the speed deviation. In addition, different control schemes for a TCSC were proposed such as variable structure controller [18,19], bilinear generalized predictive controller [20], H_∞-based controller [21], neural network controller [22], and simulated annealing based controllers [23].

In this paper, a comprehensive assessment of the effects of the excitation and TCSC control when applied independently and also through coordinated application has been carried out. The design problem is transformed into an optimization problem where the real-coded genetic algorithm (RCGA) is employed to search for the optimal settings of stabilizer parameters. A controllability measure based on singular value decomposition (SVD) is used to identify the effectiveness of each control input. In addition, the damping torque coefficient is evaluated with the proposed stabilizers over a wide range of loading conditions. For completeness, the eigenvalue analysis and nonlinear simulation results are carried out to demonstrate the effectiveness and robustness of the proposed stabilizers to enhance system stability.

2. Power system model

2.1. Generator

In this study, a single machine infinite bus system as shown in Fig. 1 is considered. The generator is equipped with PSS and the system has an TCSC at the midpoint of the line as shown in Fig. 1. The line impedance is $Z = R + \mathrm{j}X$ and the generator has a local load of admittance $Y_\mathrm{L} = g + \mathrm{j}b$. The generator is represented by the third-order model comprising of the electromechanical swing equation and the generator internal voltage equation [1,2]. The swing equation is divided into the following equations:

$$\dot{\delta} = \omega_\mathrm{b}(\omega - 1) \tag{1}$$

$$\dot{\omega} = \frac{1}{M}(P_\mathrm{m} - P_\mathrm{e} - D(\omega - 1)) \tag{2}$$

where P_m and P_e are the input and output powers of the generator, respectively; M and D the inertia constant and damping coefficient, respectively; δ and ω the rotor angle and speed, respectively; ω_b the synchronous speed. The output power of the generator can be expressed in terms of the d-axis and q-axis components of the armature current, i, and terminal voltage, v, as

$$P_\mathrm{e} = v_d i_d + v_q i_q \tag{3}$$

The internal voltage, E'_q, equation is

$$\dot{E}'_q = \frac{1}{T'_\mathrm{do}}(E_\mathrm{fd} - (x_d - x'_d)i_d - E'_q) \tag{4}$$

where E_fd is the field voltage; T'_do is the open circuit field time constant; x_d and x'_d are d-axis reactance and d-axis transient reactance of the generator, respectively.

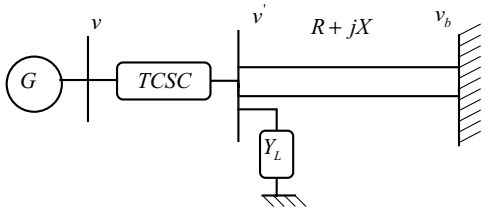

Fig. 1. Single machine infinite bus system.

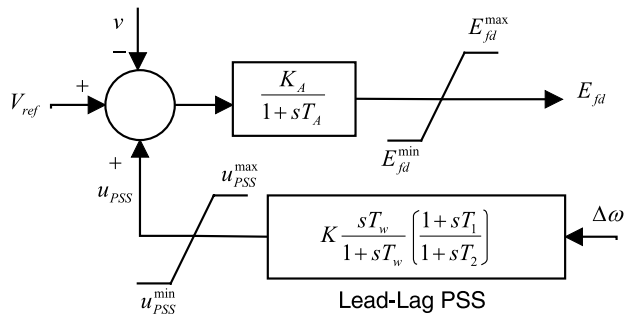

Fig. 2. IEEE type-ST1 excitation system with PSS.

2.2. Exciter and PSS

The IEEE type-ST1 excitation system shown in Fig. 2 is considered. It can be described as

$$\dot{E}_{\mathrm{fd}} = \frac{1}{T_A}(K_A(V_{\mathrm{ref}} - v + u_{\mathrm{PSS}}) - E_{\mathrm{fd}}) \tag{5}$$

where K_{A} and T_{A} are the gain and time constant of the excitation system, respectively; V_{ref} the reference voltage. As shown in Fig. 2, a conventional lead–lag PSS is installed in the feedback loop to generate a stabilizing signal u_{PSS}. In Eq. (5), the terminal voltage v can be expressed as

$$v = (v_d^2 + v_q^2)^{1/2} \tag{6}$$

$$v_d = x_q i_q \tag{7}$$

$$v_q = E'_q - x'_d i_d \tag{8}$$

where x_q is the q-axis reactance of the generator.

2.3. TCSC-based stabilizer

Fig. 3 illustrates the block diagram of a TCSC with a lead–lag compensator. The reactance of the TCSC, X_{TCSC}, can be expressed as

$$\dot{X}_{\mathrm{TCSC}} = \frac{1}{T_{\mathrm{s}}}(K_{\mathrm{s}}(X^{\mathrm{ref}}_{\mathrm{TCSC}} - u_{\mathrm{TCSC}}) - X_{\mathrm{TCSC}}) \tag{9}$$

where $X^{\mathrm{ref}}_{\mathrm{TCSC}}$ is the reference reactance of TCSC; K_{s} and T_{s} the gain and time constant of the TCSC. As shown in Fig. 3, a conventional lead–lag controller is installed in the feedback loop to generate the TCSC stabilizing signal u_{TCSC}.

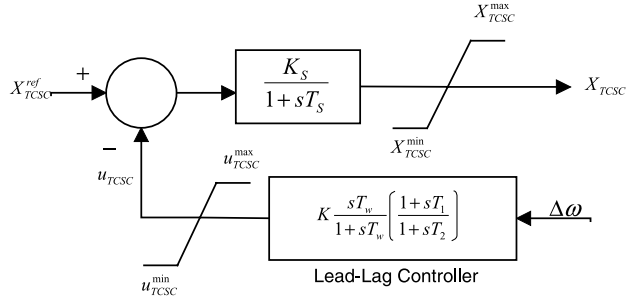

Fig. 3. TCSC with lead–lag controller.

2.4. Linearized model

In the design of electromechanical mode damping controllers, the linearized incremental model around a nominal operating point is usually employed [1,2]. Linearizing the expressions of i_d and i_q and substituting into the linear form of Eqs. (1)–(9) yield the following linearized power system model:

$$\begin{bmatrix} \Delta\dot{\delta} \\ \Delta\dot{\omega} \\ \Delta\dot{E}'_q \\ \Delta\dot{E}_{\mathrm{fd}} \end{bmatrix} = \begin{bmatrix} 0 & 377 & 0 & 0 \\ -\frac{K_1}{M} & -\frac{D}{M} & -\frac{K_2}{M} & 0 \\ -\frac{K_4}{T'_{\mathrm{do}}} & 0 & -\frac{K_3}{T'_{\mathrm{do}}} & \frac{1}{T'_{\mathrm{do}}} \\ -\frac{K_A K_5}{T_A} & 0 & -\frac{K_A K_6}{T_A} & -\frac{1}{T_A} \end{bmatrix} \times \begin{bmatrix} \Delta\delta \\ \Delta\omega \\ \Delta E'_q \\ \Delta E_{\mathrm{fd}} \end{bmatrix} + \begin{bmatrix} 0 & 0 \\ 0 & -\frac{K_p}{M} \\ 0 & -\frac{K_q}{T'_{\mathrm{do}}} \\ \frac{K_A}{T_A} & -\frac{K_A K_v}{T_A} \end{bmatrix} \times \begin{bmatrix} u_{\mathrm{PSS}} \\ \Delta X_{\mathrm{TCSC}} \end{bmatrix} \tag{10}$$

In short,

$$\dot{X} = AX + HU \tag{11}$$

where the state vector X is $[\Delta\delta, \Delta\omega, \Delta E'_q, \Delta E_{\mathrm{fd}}]^T$ and the control vector U is $[u_{\mathrm{PSS}}, \Delta X_{\mathrm{TCSC}}]^T$. The block diagram of the linearized power system model is depicted as shown in Fig. 4 where K_1–K_6, K_p, K_q, and K_v are linearization constants defined as

$$K_1 = \frac{\partial P_{\mathrm{e}}}{\partial\delta}, \quad K_2 = \frac{\partial P_{\mathrm{e}}}{\partial E'_q}, \quad K_p = \frac{\partial P_{\mathrm{e}}}{\partial X_{\mathrm{TCSC}}},$$
$$K_4 = \frac{\partial E_q}{\partial\delta}, \quad K_3 = \frac{\partial E_q}{\partial E'_q}, \quad K_q = \frac{\partial E_q}{\partial X_{\mathrm{TCSC}}}, \tag{12}$$
$$K_5 = \frac{\partial v}{\partial\delta}, \quad K_6 = \frac{\partial v}{\partial E'_q}, \quad K_v = \frac{\partial v}{\partial X_{\mathrm{TCSC}}}.$$

3. The proposed approach

3.1. Electromechanical mode identification

The state equations of the linearized model can be used to determine the eigenvalues of the system matrix A. Out of these eigenvalues, there is a mode of oscillations related to machine inertia. For the stabilizers to be effective, it is extremely important to identify the eigenvalue associated with

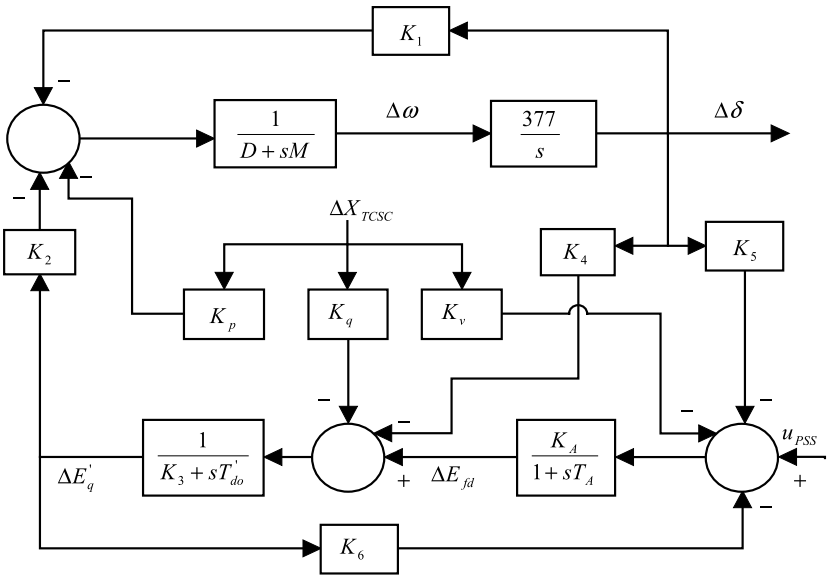

Fig. 4. Block diagram of the linearized model.

the electromechanical mode. In this study, the participation factors method [24] is used.

3.2. Controllability measure

To measure the controllability of the electromechanical mode by a given input, the singular value decomposition is employed in this study. Mathematically, if G is an $m \times n$ complex matrix then there exist unitary matrices W and V with dimensions of $m \times m$ and $n \times n$, respectively such that G can be written as

$$G = W\Sigma V^H \tag{13}$$

where

$$\Sigma = \begin{bmatrix} \Sigma_1 & 0 \\ 0 & 0 \end{bmatrix}, \quad \Sigma_1 = \mathrm{diag}(\sigma_1, \ldots, \sigma_r)$$
$$\text{with } \sigma_1 \geq \cdots \geq \sigma_r \geq 0 \tag{14}$$

where $r = \min\{m, n\}$ and $\sigma_1, \ldots, \sigma_r$ are the singular values of G.

The minimum singular value σ_r represents the distance of the matrix G from the all matrices with a rank of $r-1$. This property can be utilized to quantify modal controllability [25]. In this study, the matrix H in Eq. (11) can be written as $H = [h_1, h_2]$ where h_i is the column of matrix H corresponding to the ith input. The minimum singular value, $\sigma_{\min}$, of the matrix $[\lambda I - A\ h_i]$ indicates the capability of the ith input to control the mode associated with the eigenvalue λ. As a matter of fact, the higher the $\sigma_{\min}$, the higher the controllability of this mode by the input considered. Having been identified, the controllability of the electromechanical mode can be examined with both inputs in order to identify the most effective one to control that mode.

3.3. Stabilizer design

A widely used conventional lead–lag structure for both excitation and TCSC-based stabilizers, shown in Figs. 2 and 3, is considered. In this structure, the washout time constant T_w and the time constant T_2 are usually prespecified. The controller gain K and time constant T_1 are to be determined for each stabilizer.

In this study, several loading conditions represent nominal, light, high, and leading power factor without and with system parameter uncertainties are considered to ensure the robustness of the proposed stabilizers. In the stabilizer design process, it is aimed to maximize the damping ratio, ζ, of the poorly damped electromechanical mode eigenvalues at the entire range of the specified loading conditions. Therefore, the following eigenvalue-based objective function J is used:

$$J = \min\{\zeta_i : \zeta_i \text{ is the electromechanical mode damping ratio of the } i\text{th loading condition}\} \tag{15}$$

In the optimization process, it is aimed to *Maximize J* while satisfying the problem constraints that are the optimized parameter bounds. Therefore, the design problem can be formulated as the following optimization problem:

$$\textit{Maximize } J \tag{16}$$

Subject to

$$K^{\min} \leq K \leq K^{\max} \tag{17}$$

$$T_1^{\min} \leq T_1 \leq T_1^{\max} \tag{18}$$

$$T_3^{\min} \leq T_3 \leq T_3^{\max} \tag{19}$$

The proposed approach employs RCGA to solve this optimization problem and search for optimal or near optimal

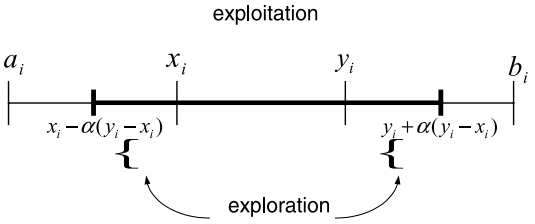

Fig. 5. Blend crossover operator (BLX-α).

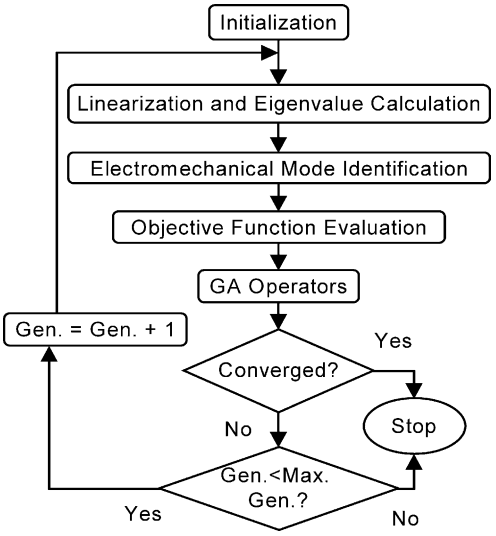

Fig. 6. Flow chart of the proposed design approach.

set of the optimized parameters. To investigate the capability of PSS and TCSC controller when applied individually and also through coordinated application, both are designed independently first and then in a coordinated manner.

3.4. Damping torque coefficient calculation

To assess the effectiveness of the designed stabilizers, the damping torque coefficient is evaluated and analyzed. The torque can be decomposed into synchronizing and damping components as follows:

$$\Delta T_e(t) = K_{syn}\,\Delta\delta(t) + K_d\,\Delta\omega(t) \tag{20}$$

where K_{syn} and K_d are the synchronizing and damping torque coefficients, respectively. It is worth mentioning that K_d is a damping measure to the electromechanical mode of oscillations [26].

In order to calculate K_{syn} and K_d, the error between the actual torque deviation and that obtained by summing both components can be defined as

$$E(t) = \Delta T_e(t) - (K_{syn}\,\Delta\delta(t) + K_d\,\Delta\omega(t)) \tag{21}$$

Then K_{syn} and K_d are computed to minimize the sum of the squared errors over the simulation period t_{sim} as

$$\sum_{i=1}^{N}[E_i]^2 = \sum_{i=1}^{N}[\Delta T_{e_i} - (K_{syn}\,\Delta\delta_i + K_d\,\Delta\omega_i)]^2 \tag{22}$$

where $t_{sim} = N \times T_{samp}$, T_{samp} is the sampling period. Thus, these coefficients should satisfy

$$\frac{\partial}{\partial K_{syn}}\sum_{i=1}^{N}[E_i]^2 = 0 \quad \text{and} \quad \frac{\partial}{\partial K_d}\sum_{i=1}^{N}[E_i]^2 = 0 \tag{23}$$

That yields

$$\sum_{i=1}^{N}\Delta T_{e_i}\,\Delta\delta_i = K_{syn}\sum_{i=1}^{N}[\Delta\delta_i]^2 + K_d\sum_{i=1}^{N}[\Delta\omega_i\,\Delta\delta_i] \tag{24}$$

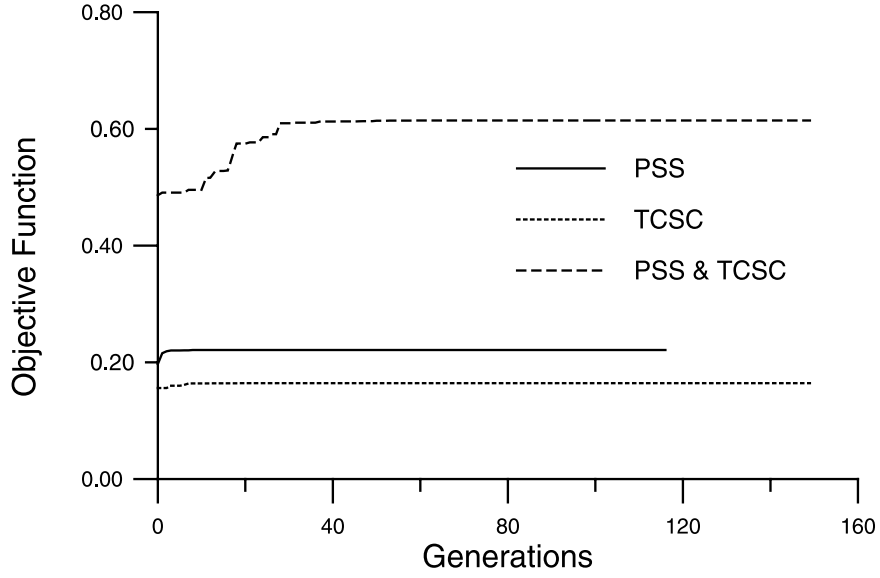

Fig. 7. Objective function convergence.

$$\sum_{i=1}^{N} \Delta T_{e_i} \Delta\omega_i = K_d \sum_{i=1}^{N} [\Delta\omega_i]^2 + K_{syn} \sum_{i=1}^{N} [\Delta\omega_i \Delta\delta_i] \quad (25)$$

Solving Eqs. (24) and (25), K_{syn} and K_d can be calculated.

4. Implementation

4.1. Real-coded genetic algorithm

Genetic algorithms (GA) are search algorithms based on the mechanics of natural selection and survival-of-the-fittest. One of the most important features of the GA as a method of control system design is the fact that minimal knowledge of the plant under investigation is required. Since the GA optimize a performance index based on input/output relationships only, far less information than other design techniques is needed. Further, because the GA search is directed towards increasing a specified performance, the net result is a controller which ultimately meets the performance criteria. In addition, because the GA do not need an explicit mathematical relationship between the performance of the system and the search update, the GA offer a more general optimization methodology than conventional analytical techniques.

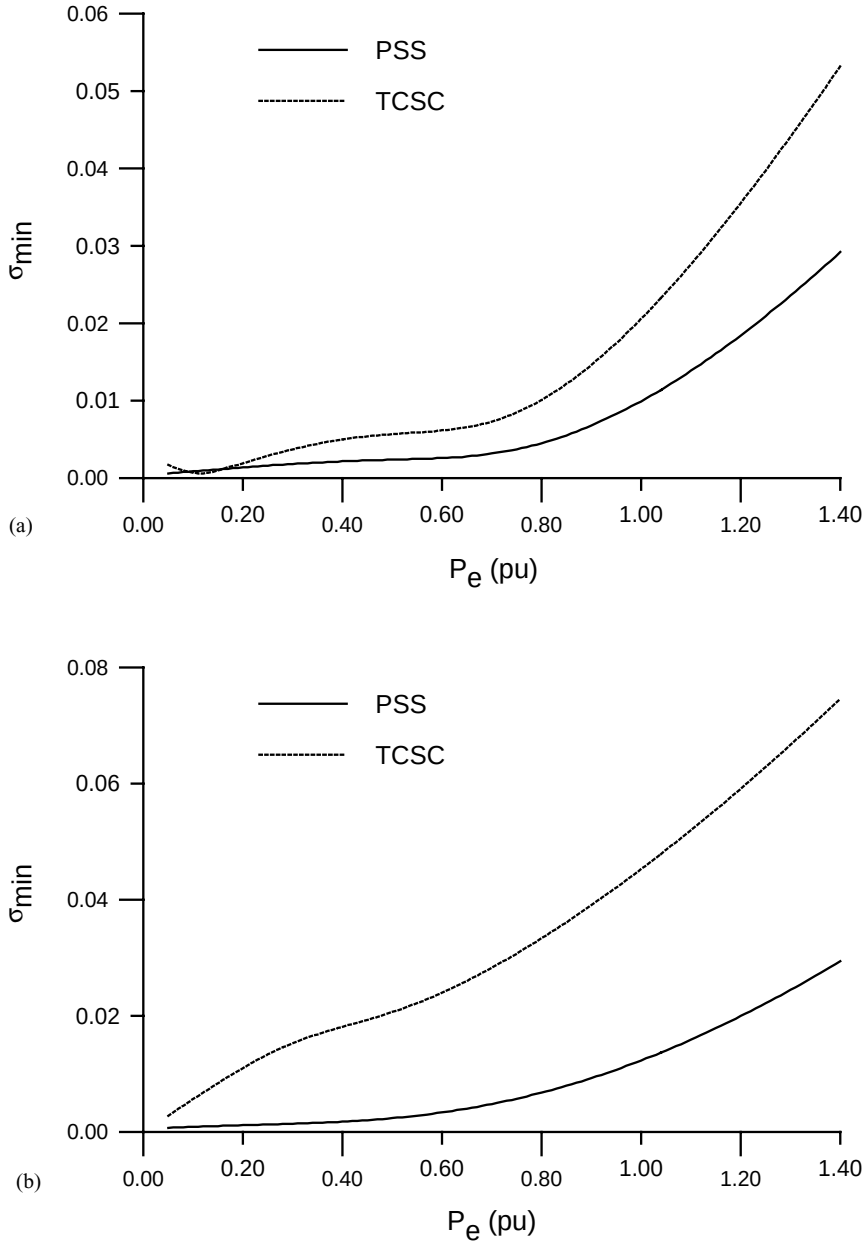

Fig. 8. Minimum singular value with loading variations. (a) $Q = -0.4$ pu; (b) $Q = 0.0$ pu; (c) $Q = 0.4$ pu.

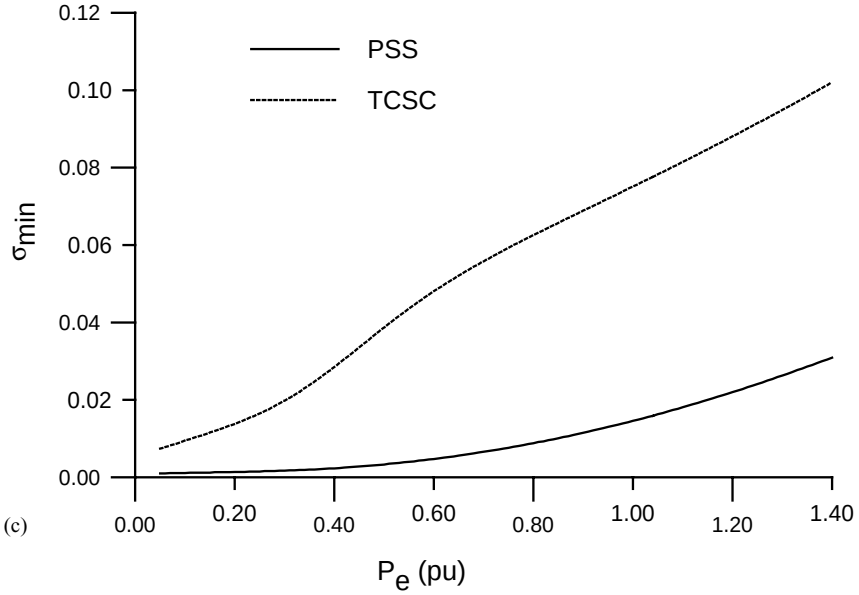

(c)

Fig. 8. (*Continued*).

Due to difficulties of binary representation when dealing with continuous search space with large dimension, the proposed approach has been implemented using real-coded genetic algorithm [27]. A decision variable x_i is represented by a real number within its lower limit a_i and upper limit b_i, i.e. $x_i \in [a_i, b_i]$. The RCGA crossover and mutation operators are described as follows:

Crossover: A blend crossover operator (BLX-α) has been employed in this study. This operator starts by choosing randomly a number from the interval $[x_i - \alpha(y_i - x_i), y_i + \alpha(y_i - x_i)]$, where x_i and y_i are the ith parameter values of the parent solutions and $x_i < y_i$. To ensure the balance between exploitation and exploration of the search space, $\alpha = 0.5$ is selected. This operator is depicted in Fig. 5.

Mutation: The non-uniform mutation operator has been employed in this study. In this operator, the new value x_i' of the parameter x_i after mutation at generation t is given as

$$x_i' = \begin{cases} x_i + \Delta(t, b_i - x_i) & \text{if } \tau = 0 \\ x_i - \Delta(t, x_i - a_i) & \text{if } \tau = 1 \end{cases} \quad (26)$$

$$\Delta(t, y) = y(1 - r^{(1-(t/g_{\max}))^{\beta}}) \quad (27)$$

where τ is a binary random number, r a random number $r \in [0, 1]$, $g_{\max}$ the maximum number of generations, and β a positive constant chosen arbitrarily. In this study, $\beta = 5$ was selected. This operator gives a value $x_i' \in [a_i, b_i]$ such that the probability of returning a value close to x_i increases as the algorithm advances. This makes uniform search in the initial stages where t is small and very locally at the later stages.

4.2. RCGA application

Linearizing the system model at each loading condition of the specified range, the electromechanical mode is identified and its damping ratio is calculated. Then, the objective function is evaluated and RCGA is applied to search for optimal settings of the optimized parameters of the proposed control schemes. In our implementation, the crossover and mutation probabilities of 0.9 and 0.01, respectively, are found to be quite satisfactory. The number of individuals in each generation is selected to be 100. In addition, the search

Table 1
Loading conditions and parameter uncertainties

Loading condition (P, Q) (pu)	Parameter uncertainties
Nominal (1.0, 0.015)	No parameter uncertainty
Light (0.3, 0.100)	The 30% increase of line reactance X
Heavy (1.1, 0.100)	The 30% decrease of field time constant T'_{do}
Leading pf (0.7, −0.300)	The 25% decrease of machine inertia M

Table 2
Optimal parameter settings of the proposed stabilizers

Individual design		Coordinated design	
PSS	TCSC	PSS	TCSC
K			
17.849	99.848	47.906	90.411
T_1			
0.4334	0.0596	0.1211	0.3080
T_2			
0.1000	0.1000	0.1000	0.1000

will terminate if the best solution does not change for more than 50 generations or the number of generations reaches 500. The computational flow chart of the proposed design approach is shown in Fig. 6.

5. Results and discussions

5.1. Loading conditions and proposed stabilizers

In this study, the PSS and TCSC-based controller parameters are optimized over a wide range of operating conditions and system parameter uncertainties. Four loading conditions represent nominal, light, heavy, and leading power factor are considered. Each loading condition is considered without and with parameter uncertainties as given in Table 1. Hence, the total number of points considered for the design process is 16.

The proposed approach has been implemented on a weakly connected power system. The detailed data of the power system used in this study is given in [1]. The convergence rate of the objective function J when PSS and TCSC controller designed individually and through coordinated design is shown in Fig. 7. It can be seen that the damping characteristics of the coordinated design approach are much better than those of the individual design one. The final settings of the optimized parameters for the proposed stabilizers are given in Table 2.

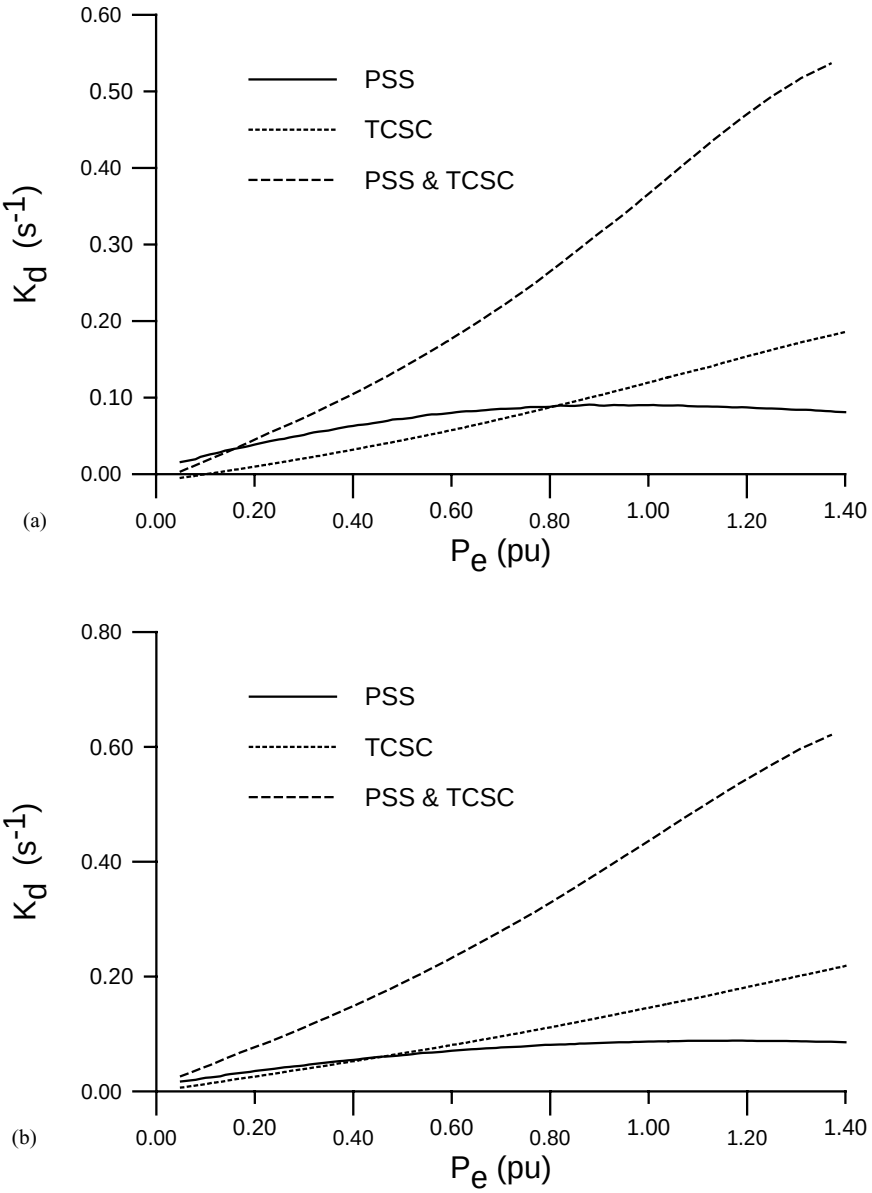

Fig. 9. Damping coefficient with the loading variations. (a) $Q = -0.4$ pu; (b) $Q = 0.0$ pu; (c) $Q = 0.4$ pu.

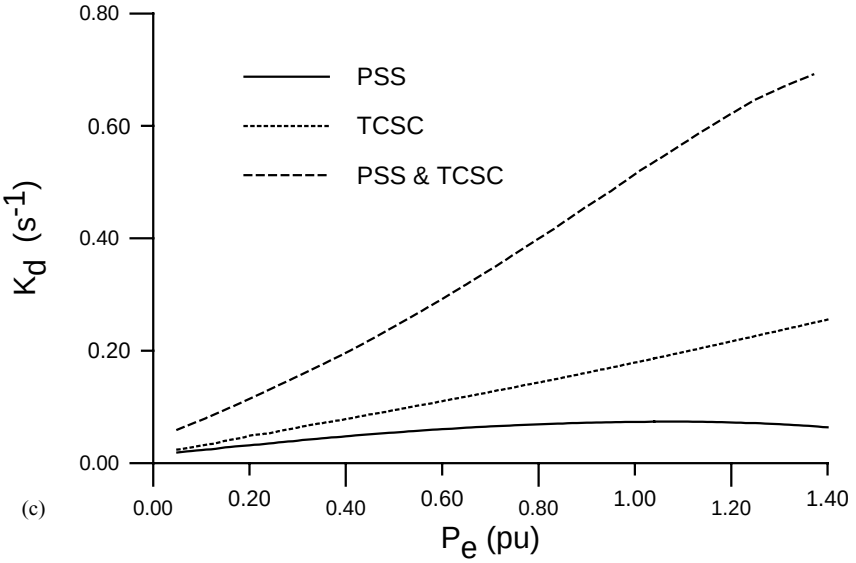

Fig. 9. (*Continued*).

5.2. Mode controllability measure

With each input signal, the minimum singular value $\sigma_{\min}$ has been estimated to measure the controllability of the electromechanical mode from that input. Fig. 8 shows $\sigma_{\min}$ with loading conditions over the range of $P_e = [0.05–1.4]$ pu and $Q \in \{-0.4, 0.0, 0.4\}$ pu. At each loading condition in the specified range, the system model is linearized, the electromechanical mode is identified, and the SVD-based controllability measure is implemented. It can be seen that the electromechanical mode controllability through TCSC is much more effective than the case of PSS. This feature is more evident with heavily loading conditions.

5.3. Damping torque coefficient

In order to evaluate the effectiveness of the proposed stabilizers, the damping torque coefficient has been estimated with PSS and TCSC-based stabilizer when designed individually and in coordinated manner. Fig. 9 shows K_d versus the loading variations with PSS only, TCSC-based stabilizer only, and coordinated PSS and TCSC-based

Table 3
System eigenvalues with the proposed stabilizers at nominal loading

No control	PSS only	TCSC only	Coordinated design
+0.2954 ± j4.9569, −0.0595*	−3.2392 ± j8.9962, 0.3388*	−3.2798 ± j3.9564, 0.6384*	−4.8776 ± j2.7684, 0.8697*
−10.3930 ± j3.2870	−1.7990 ± j3.5181	−6.0400 ± j7.2847	−12.3566 ± j18.0598
–	−20.1152	−19.1942	−13.0216
–	−0.2041	−12.3529	−10.0000
–	–	−0.2090	−2.6828
–	–	–	−0.2227
–	–	–	−0.2000

Table 4
System eigenvalues with the proposed stabilizers at light loading

No control	PSS only	TCSC only	Coordinated design
−0.0090 ± j4.8503, 0.0019*	−1.1586 ± j4.6742, 0.2406*	−0.8464 ± j5.1193, 0.1631*	−2.9009 ± j4.6338, 0.5306*
−10.0888 ± j3.8341	−5.4717 ± j6.2645	−9.8644 ± j3.8594	−15.4225 ± j6.3016
–	−16.9332	−19.7018	−6.7704 ± j4.2023
–	−0.2017	−9.0691	−10.0000
–	–	−0.2031	−0.2081
–	–	–	−0.2000

Table 5
System eigenvalues with the proposed stabilizers at heavy loading

No control	PSS only	TCSC only	Coordinated design
+0.4852 ± j3.6903, −0.1304*	−1.1692 ± j3.5341, 0.3141*	−6.0777 ± j8.0732, 0.6014*	−9.3541 ± j2.4209, 0.9681*
−11.5830 ± j3.6960	−4.8014 ± j6.5925	−18.8429	−12.9142 ± j20.7924
–	−18.2475	−10.3699	−10.000
–	−0.2070	−6.3952	−4.5495
–	–	−2.4054	−1.0485
–	–	−0.2269	−0.2610
–	–	–	−0.2000

stabilizer. It was observed that the TCSC provides negative damping at low loading conditions in particular with leading power factor loading. This problem is alleviated with the coordinated design approach. It can be also seen that PSS outperforms TCSC and does not suffer from such a prblem. It is also evident that the coordinated design of PSS and TCSC-based stabilizer provides great damping characteristics and enhance significantly the system stability compared to individual design of these stabilizers.

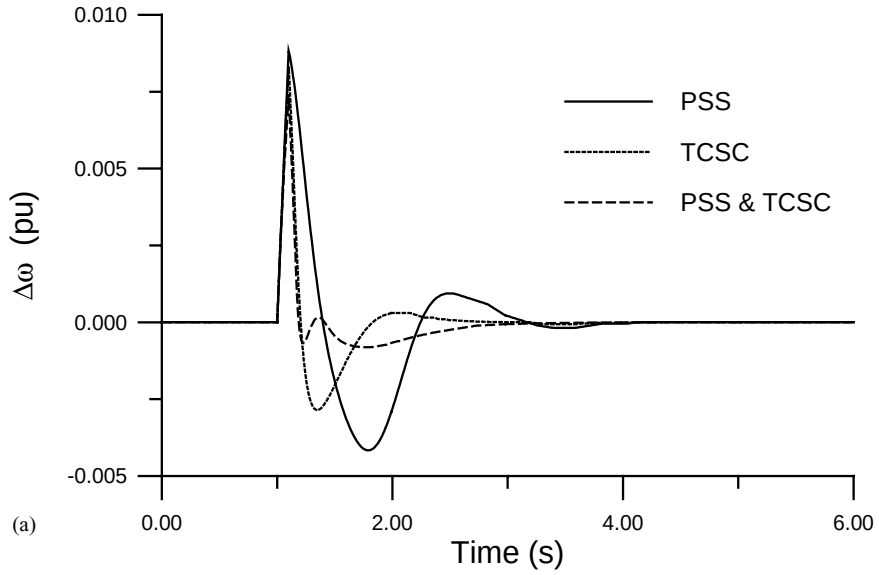

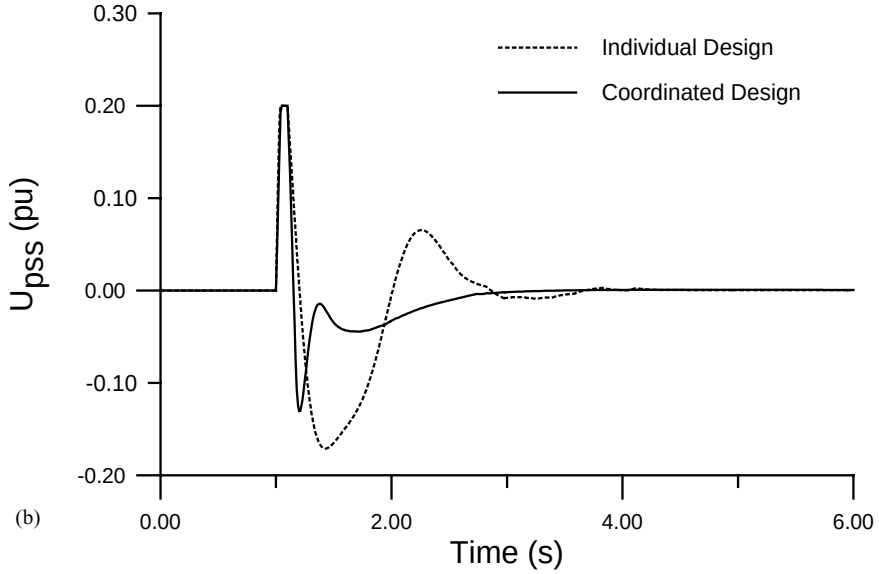

Fig. 10. System response for a six-cycle fault disturbance with nominal loading. (a) Rotor speed response; (b) PSS stabilizing signal; (c) X_{TCSC} variation.

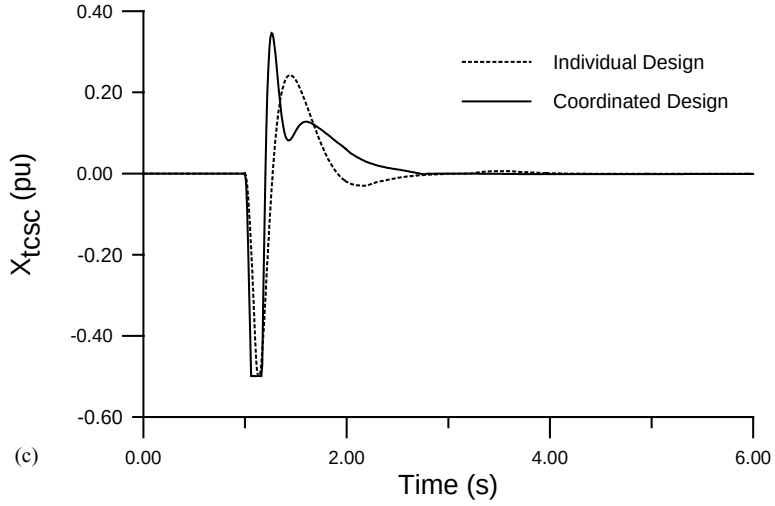

Fig. 10. (*Continued*).

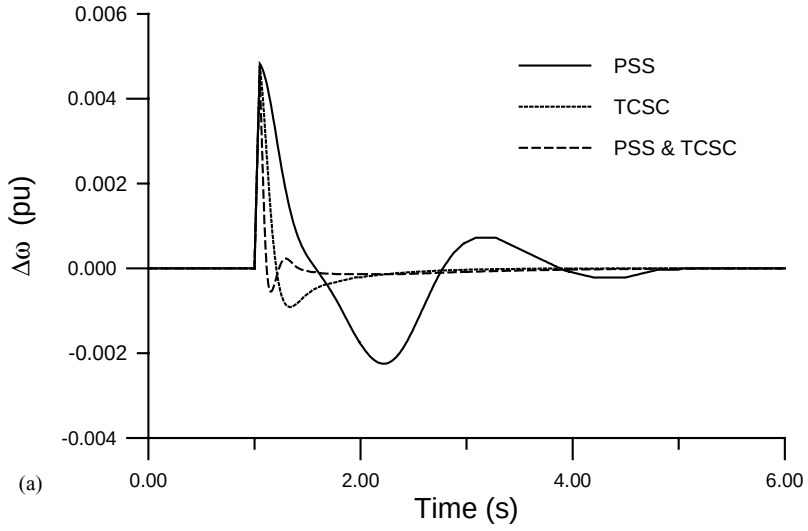

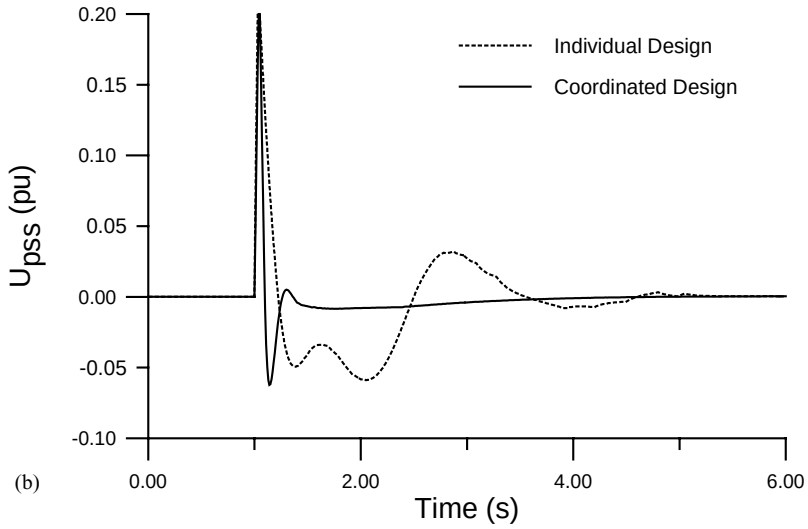

Fig. 11. System response for a three-cycle fault disturbance with heavy loading. (a) Rotor speed response; (b) PSS stabilizing signal; (c) X_{TCSC} variation.

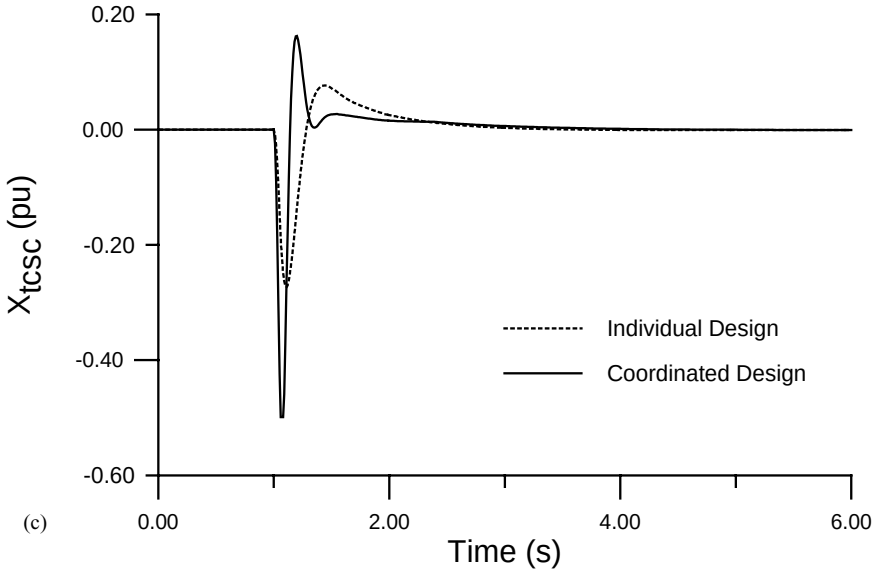

(c)

Fig. 11. (*Continued*).

5.4. Eigenvalue analysis and nonlinear simulations

For completeness and verification, all the proposed stabilizers were tested at the following disturbances and loading conditions:

(a) Nominal loading $(P, Q) = (1.0, 0.015)$ pu with six-cycle three-phase fault.
(b) Light loading $(P, Q) = (0.3, 0.015)$ pu with six-cycle three-phase fault.
(c) Heavy loading $(P, Q) = (1.1, 0.4)$ pu with three-cycle three-phase fault.

The system eigenvalues without and with the proposed stabilizers at these loading conditions are given in Tables 3–5, respectively, where the first row represents the electromechanical mode eigenvalues and their damping ratios. It is clear that the system stability is greatly enhanced with the proposed stabilizers. It can be also seen that the coordinated design outperforms the individual design at all points considered in the sense that the damping ratios and damping factors of the electromechanical modes at all points are greatly improved.

The nonlinear time domain simulations have been carried out at the disturbances and the loading conditions specified above. Fig. 10 shows the system response with a six-cycle fault disturbance at the nominal loading condition. It can be seen that the coordinated design approach provides the best damping characteristics and enhance greatly the first swing stability. The stabilizing signal of PSS, U_{PSS}, and the reactance of the TCSC, X_{TCSC}, when designed individually and in coordinated manner are compared and shown in Fig. 10b and c, respectively. It is clear that the control effort is greatly reduced with the coordinated design approach.

Fig. 11 shows the results with a three-cycle fault disturbance at a heavy loading condition. It is clear that the first swing stability is greatly improved with the coordinated design approach. This confirms the findings of Fig. 9. The proposed schemes outperform the CPSS and the control efforts are significantly reduced. This confirms the potential of the proposed approach for ultimate utilization of the control schemes to enhance the system dynamic stability.

6. Conclusion

In this study, the power system stability enhancement via PSS and TCSC-based stabilizer when applied independently and also through coordinated application was discussed and investigated. For the proposed stabilizer design problem, an eigenvalue-based objective function to increase the system damping was developed. Then, the real-coded genetic algorithm was implemented to search for the optimal stabilizer parameters. In addition, a controllability measure for the poorly damped electromechanical modes using a singular value decomposition approach was used to assess the effectiveness of the proposed stabilizers. The damping characteristics of the proposed schemes were also evaluated in terms of the damping torque coefficient. The proposed stabilizers have been tested on a weakly connected power system with different loading conditions. The eigenvalue analysis and nonlinear simulation results show the effectiveness and robustness of the proposed stabilizers to enhance the system stability.

Acknowledgements

The authors acknowledge the support of King Fahd University of Petroleum and Minerals via funded Project # FT/2000-25.

References

[1] Y.N. Yu, Electric Power System Dynamics, Academic Press, New York, 1983.
[2] P.W. Sauer, M.A. Pai, Power System Dynamics and Stability, Prentice-Hall, Englewood Cliffs, NJ, 1998.
[3] T.C. Yang, Applying H_∞ optimisation method to power system stabilizer design parts 1&2, Int. J. Electrical Power Energy Syst. 19 (1) (1997) 29–43.
[4] R. Asgharian, A robust H_∞ power system stabilizer with no adverse effect on shaft torsional modes, IEEE Trans. Energy Convers. 9 (3) (1994) 475–481.
[5] M. Vidyasagar, H. Kimura, Robust controllers for uncertain linear multivariable systems, Automatica 22 (1) (1986) 85–94.
[6] H. Kwakernaak, Robust control and H_∞ optimization-tutorial, Automatica 29 (2) (1993) 255–273.
[7] P. Kundur, M. Klein, G.J. Rogers, M.S. Zywno, Application of power system stabilizers for enhancement of overall system stability, IEEE Trans. PWRS 4 (2) (1989) 614–626.
[8] M.J. Gibbard, Robust design of fixed-parameter power system stabilizers over a wide range of operating conditions, IEEE Trans. PWRS 6 (2) (1991) 794–800.
[9] Y.L. Abdel-Magid, M.A. Abido, S. Al-Baiyat, A.H. Mantawy, Simultaneous stabilization of multimachine power systems via genetic algorithms, IEEE Trans. PWRS 14 (4) (1999) 1428–1439.
[10] N.G. Hingorani, Flexible AC Transmission, IEEE Spectrum, April 1993, pp. 40–45.
[11] N.G. Hingorani, FACTS-flexible ac transmission system, in: Proceedings of the Fifth International Conference on AC and DC Power Transmission, vol. 345, IEE Conference Publication, 1991, pp. 1–7.
[12] M. Noroozian, G. Anderson, Damping of power system oscillations by use of controllable components, IEEE Trans. PWRD 9 (4) (1994) 2046–2054.
[13] H.F. Wang, F.J. Swift, A unified model for the analysis of FACTS devices in damping power system oscillations. Part I. Single-machine infinite-bus power systems, IEEE Trans. PWRD 12 (2) (1997) 941–946.
[14] M.A. Abido, Y.L. Abdel-Magid, Analysis and design of power system stabilizers and facts based stabilizers using genetic algorithms, in: Proceedings of the Power System Computation Conference PSCC-2002, Paper #360, Spain, 24–28 June 2002.
[15] X. Chen, N. Pahalawaththa, U. Annakkage, C. Kumble, Controlled series compensation for improving the stability of multimachine power systems, IEE Proc. 142 (Pt. C) (1995) 361–366.
[16] J. Chang, J. Chow, Time optimal series capacitor control for damping inter-area modes in interconnected power systems, IEEE Trans. PWRS 12 (1) (1997) 215–221.
[17] T. Lie, G. Shrestha, A. Ghosh, Design and Application of Fuzzy Logic Control Scheme for Transient Stability Enhancement in Power Systems, Electric Power Systems Research, 1995, pp. 17–23.
[18] Y. Wang, R. Mohler, R. Spee, W. Mittelstadt, Variable structure FACTS controllers for power system transient stability, IEEE Trans. PWRS 7 (1992) 307–313.
[19] T. Luor, Y. Hsu, Design of an output feedback variable structure thyristor controlled series compensator for improving power system stability, Electric Power Syst. Res. 47 (1998) 71–77.
[20] V. Rajkumar, R. Mohler, Bilinear generalized predictive control using the thyristor controlled series capacitor, IEEE Trans. PWRS 9 (4) (1994) 1987–1993.
[21] Q. Zhao, J. Jiang, A TCSC damping controller using robust control theory, Int. J. Electric Power Syst. Res. 20 (1) (1998) 25–33.
[22] X. Dai, J. Liu, Y. Tang, N. Li, H. Chen, Neural network αth-order inverse control of thyristor controlled series compensator, Electric Power Syst. Res. 45 (1998) 19–27.
[23] M.A. Abido, Pole placement technique for PSS and TCSC-based stabilizer design using simulated annealing, Int. J. Electric Power Syst. Res. 22 (8) (2000) 543–554.
[24] Y.Y. Hsu, C.L. Chen, Identification of optimum location for stabilizer applications using participation factors, IEE Proc. 134 (3) (Pt. C) (1987) 238–244.
[25] A.M.A. Hamdan, An investigation of the significance of singular value decomposition in power system dynamics, Int. J. Electric Power Syst. Res. 21 (1999) 417–424.
[26] E. A Failat, M. Bettayyeb, H. Al-Duwaish, M.A. Abido, A. Mantawy, A neural network based approach for on-line dynamic stability assessment using synchronizing and damping torque coefficients, Electric Power Syst. Res. 39 (2) (1996) 103–110.
[27] F. Herrera, M. Lozano, J.L. Verdegay, Tackling real-coded genetic algorithms: operators and tools for behavioral analysis, Artif. Intell. Rev. 12 (4) (1998) 265–319.